Growth Factors and Other Bioactive Molecules for PPF Tissue Engineered Bone Implants

Honors Research Thesis

Presented in Partial Fulfillment of the requirements for graduation with honors research distinction in the undergraduate colleges of The Ohio State University

By

Ryan Sefcik

The Ohio State University

April 2016

Project Advisor: Dr. David Dean Ph.D., Department of Plastic Surgery

Table of Contents

Background 3

Primary Aims of Project 7

Materials and Methods 8

Materials 8

Frequently Utilized Techniques 9

I. Washing/ Sterilization Methods for PPF scaffolds 9

II. Cell Culture 10

III. MTT assay 11

IV. SEM analysis 11

V. Toluidine blue assay 11

VI. Qualitative ALP Staining 12

VII. Quantitative ALP Assay 13

VIII. Alizarin Red S Staining 13

IX. Alizarin Red S Assay 13

Experiment Methods – Two Dimensional Study 14

I. Fabrication of Thin Film Two-Dimensional Scaffolds 14

II. Preliminary Study: Cytotoxicity 14

III. Preliminary Study: Cell Seeding Density 15

IV. Growth Factor Literature Review for ECM Study 15

V. Extracellular Matrix (ECM) Study 16

Experiment Methods – Three-Dimensional Study 17

I. Fabrication of Three-Dimensional Porous Scaffolds 17

II. Replication of Two-Dimensional Findings on Three-Dimensional Scaffolds 17

Results and Discussions – Two Dimensional Study 18

Determination of Cell Seeding Density 18

Analysis of Cell Proliferation 18

I. MTT Assay 18

II. Toluidine Blue Staining 19

III. SEM imaging and analysis 19

Analysis of hMSC differentiation 19

I. Alkaline Phosphatase Assay and Stain 19

II. Alizarin Red S Assay and Stain for Bone Mineralization 20

III. SEM Analysis for Cell Differentiation 21
Results and Discussions - Three-Dimensional Study 21
Analysis of hMSC proliferation and Coating 21
I. SEM Analysis for Cell Proliferation and Coating 21
Final Conclusions 22
Future Work 22
Three-Dimensional Study 22
Defined Media Study 22
Other Work 23
Acknowledgments 24
References 25
Figures 32

Background

The repair of bone defects and deficiencies due to trauma, cancer, birth defects, or aging are an interesting and important area of study for bone tissue engineering. The high demand for functional bone grafts has led to the search for artificial bone substitutes. Traditionally, non-resorbable, inert metals and other rigid materials have been implemented for repairing bone defects [1-3]. However, these rigid materials do not allow for the appropriate and natural distribution of stresses and may lead to stress shielding [4]. Stress shielding is defined as the loss of bone density, and therefore strength, as a result of the removal of normal stress conditions on the bone caused by the presence of the implant [5]. Bone tissue engineering is the area of study which seeks to overcome the disadvantages and limitations of current approaches for bone repair by using regeneration-based methods combining biomaterials, cells, and growth factors [6].

The following biomaterials are commonly used for bone tissue engineering applications: polymers, ceramics, bioactive glass, composites of polymers and ceramics, and resorbable metals. Some polymers used for repairing bone defects include: poly(lactic acid) (PLA), poly(glycolic acid) (PGA), poly(caprolactone) (PCL), poly(propylene fumurate) (PPF), hyaluronic acid, chitosan, collagen, etc. [7]. Bioceramics frequently used for bone tissue engineering are hydroxyapatite (HA), calcium phosphate, and bioactive glasses containing silicate, calcium, phosphorus and sodium, and other bioactive inorganic materials [8]. The original bioactive glass is known as Bioglass 45S5 and contains 45% wt % SiO_2, 24.5% wt % Na_2O, 24.5 wt % CaO, and 6 wt % P_2O_5. [8]. Other bioactive glasses studied over the years contain elements such as fluorine, magnesium, strontium, iron, and others. In addition, many composites of polymers and bioactive glasses or ceramics have been attempted. [9].

Metals and metal alloys have also been commonly used as bone grafts. Some of the most used metals include stainless steel, vitallium, tantalum, and titanium [44]. Metals are useful in that they can be shaped, made porous, or used as coatings [45]. The porous structures allow for rapid ingrowth in bone grafts [45]. The main downside to using metals for bone grafts is that they will remain in the recipient and, as a result, may lead to the phenomenon of stress shielding [4].

Of the polymers and other materials listed above, PPF will be explored for its biodegradable, resorbable, and photocrosslinkable capabilities [10-16]. It has the ability to be 3D printed as a porous structure using ultra-violet (UV) light, photoinitiators such as Irgacure 819 (BAPO), Irgacure 784, and light-absorber 2- Hydroxy-4-methoxybenzophenone (HMB), etc [13, 15-17]. In addition, PPF, when crosslinked, exhibits advantageous properties of good mechanical strength and biocompatibility [13, 15-17]. Material biocompatibility and suitability for cell attachment, proliferation, and differentiation is of the utmost importance because cell death occurs in cytotoxic environments [18].

Bone marrow derived human mesenchymal stem cells (BM-hMSCs) are the most commonly used cells for bone tissue engineering applications. They are one of the most favorable progenitor cells because of their immunomodulatory potential upon implantation into the body [19-22]. BM-hMSCs are expected to present very low to medium amounts of human leukocyte antigens (HLA, aka MHC class II antigens) so that they are not recognized as foreign cells and therefore, are not rejected by the recipient. BM-hMSCs ability to evade the host immune system allows them to modulate the surrounding environment and be useful as allogeneic cell sources for human application until these stem cells have matured into osteocytes [20]. Allogenic therapeutic approaches use tissues from non-identical people instead of tissues or

even proteins from one part of the body to another in the same individual [43]. Allografts allow the recipient individual can receive a bone graft without needing to take tissue or cells from another part of their body [43]. For this reason, the ideal application is to differentiate BM-hMSCs to osteoblasts but not all the way to mature osteocytes, which would present HLAs. This allows cell seeded scaffolds to be implanted into the recipient's body with little risk of rejection.

Other cell types that have been studied for bone tissue engineering applications include fibroblasts, adipose derived MSCs, muscle derived MSCs, pluripotent MSCs, embryonic MSCs, and induced pluripotent MSCs. However, these cell types present high levels of cell surface antigens and thus lack the ability to evade the host immune system. Due to their lack of cell surface antigens and for their ease of proliferation and differentiation into osteoblasts, BM-hMSCs have become the most commonly used cell type for bone tissue engineering.

The use of bioactive molecules such as growth and differentiation factors, adhesion peptides, and osteotrophic drugs [23] has been explored at length regarding bone tissue engineering and regenerative medicine in general. The *in vivo* environment of skeletal formation is rich in molecules that stimulate cell adhesion, proliferation, migration, differentiation, osteogenesis, and vascularization. Growth factors can be introduced at different times to induce desired outcomes such as proliferation and differentiation. For example, proliferation can be induced using one growth factor regime and then, differentiation of the cells can be caused by switching to a different growth factor regime. Growth factors commonly used for proliferation of BM-hMSCs include Fibroblast Growth Factor (FGF), Platelet-Derived Growth Factor (PDGF-b), Epidermal Growth Factor (EGF), and Vascular Endothelial Growth Factor (VEGF) [24-27]. Commonly used growth factors for osteogenic differentiation of BM-hMSCs include bone morphogenetic protein (BMP)-2, BMP-4, BMP-6, BMP-7, and other growth differentiation

factors (GDFs) [28-36]. Different methods have been used for introducing growth factors, including introduction to the cell environment via solubilization of growth factors in the cell culture medium. Additionally, growth factors should only be used at the *in vitro* level because *in vivo* exposure to growth factors can lead to unfavorable, dangerous outcomes such as malignancy, pain, unwanted differentiation, and teratogenicity [37, 38]. Prior studies that introduced BMPs *in vivo* have demonstrated unfavorable outcomes, such as uncontrolled bone formation [37].

Commercial media are available for the proliferation and differentiation of MSCs into osteoblasts through companies such as Lonza, RoosterBio, OH-Alive, and many others. However, such media are expensive and the exact compositions are proprietary and therefore unknown to the user. Therefore, development of a defined media which acts as effectively as the commercial media for bone tissue engineering applications would be beneficial to future work, especially clinical trials, because of FDA requirements that tightly monitor and control the use of growth factors and other bioactive molecules.

We hypothesize that proliferation and differentiation can be achieved through the combination of growth factors and a suitable biocompatible material. This environment will allow BM-hMSCs to coat PPF scaffolds and subsequently secrete sufficient bone ECM for bone tissue engineering applications. Additionally, we hypothesize that the growth factor regime will be effective in achieving bone ECM on both 2D thin film scaffolds and 3D porous scaffolds. Scaffolds covered in bone ECM can act as artificial bone tissue engineered grafts because the host bone tissue can recognize the graft, leading to bone regeneration. We aim to optimize dosage of growth factors for coating PPF biomaterials with bone ECM. Our growth factor doses were chosen based on a careful literature search. However, an optimum dose has yet to be

determined and reported in literature. The following paper will discuss the results of different growth factor doses and osteogenic factors for proliferation and osteoblastic differentiation of BM-hMSCs. An optimum dose has been determined as a result of the findings of this work. We also hypothesize that our growth factor dose will work as well or better than commercially available media. Finally, the smooth translation of 2D to 3D results will be shown through replication of the optimized growth factor regimens on 3D printed, porous scaffolds.

Primary Aims of Project

The following thesis has three main objectives:

1) Determine the appropriate growth factor regimen and doses for proliferation and differentiation of BM-hMSCs.

Prior to beginning the study, careful review of the literature was necessary to determine which growth factors to use and what dosages to try. When looking at growth factors, the most important characteristics were induction of proliferation and osteogenic differentiation of BM-hMSCs, safety/ controllability, dosage, and cost. Additionally, previous work with FGF, PDGF, and BMP-7 completed by the Osteo Engineering Lab contributed to the determination of the regimens.

2) Achieve a mineralized, bone ECM layer on 2D thin film scaffolds using determined growth factor regimens.

2D thin films with an area of 1 cm^2 are very simple scaffold structures. Achievement of a mineralized, bone ECM layer on the 2D thin films was necessary prior to attempting to do the same on complex, 3D, porous scaffold geometry. Additionally, methods of analysis are typically easier to perform on the thin film scaffolds. Therefore, we first attempted the study on thin film scaffolds for their simplicity in fabrication, cell culturing, and analysis.

3) Validate the results from the 2D thin film scaffolds on 3D scaffold geometry.

Lastly, it is important to show that the 2D thin film scaffold results could be replicated on 3D, porous scaffolds. This is specifically important because bone implants will ultimately be 3D and porous. Showing that an ECM layer can be achieved throughout a 3D scaffold shows that our growth factor regime and technique is not limited by structure type. Additionally, future work will aim to replicate the outcomes on abnormal or irregularly shaped implants. This is especially important because the current goal of the Osteo Engineering Lab is to create patient-specific bone tissue engineered implants. Therefore, ensuring that we can achieve an ECM layer on any scaffold is a must for future projects.

Materials and Methods

Materials

hMSC (MSC-001, RoosterBio Inc., Frederick, MD), RoosterBio hMSC Differentiation Basal Medium (KT-004, RoosterBio Inc., Frederick, MD), LIVE/DEAD® Viability/Cytotoxicity Kit, for mammalian cells (Life Technologies, Grand Island, NY, USA), 0.25% Trypsin-EDTA (Life Technologies, Grand Island, NY, USA), MTT reagent (Sigma-Aldrich, St. Louis, MO, USA), DMSO (VWR, Radnor, PA, USA), PBS (Life Technologies, Grand Island, NY, USA), Acetone (VWR, Radnor, PA, USA), Ethanol (Fisher Scientific, Pittsburgh, PA, USA), toluidine blue (Sigma-Aldrich, St. Louis, MO, USA), FGF, PDGF-BB and EGF (PeproTech, Rocky Hill, NJ, USA), 2-Hydroxy-4-methoxybenzophenone (Sigma-Aldrich, St. Louis, MO, USA), Irgacure 784 (BASF, Florham Park, NJ, USA), Irgacure 819 (BASF, Florham Park, NJ, USA), Sodium tetraborate (Sigma-Aldrich, St. Louis, MO, USA), Formaldehyde solution (Sigma-Aldrich, St. Louis, MO, USA), Triton X-100 (Sigma-Aldrich, St. Louis, MO, USA), Bovine Serum Albumin (Life technologies, Grand Island, NY, USA), Alizarin Red S (Sigma-Aldrich, St. Louis, MO,

USA), Cetylpyridinium Chloride (Sigma-Aldrich, St. Louis, MO, USA), Fast Violet B (Sigma-Aldrich, St. Louis, MO, USA), p-nitrophenol phosphate tablets (Sigma-Aldrich, St. Louis, MO, USA), Mayer's Hematoxylin Solution (Sigma-Aldrich, St. Louis, MO, USA), Napthol AS-MX Phosphate Alkaline Solution (Sigma-Aldrich, St. Louis, MO, USA), Sodium phosphate monobasic monohydrate (Sigma-Aldrich, St. Louis, MO, USA), Sodium phosphate dibasic heptahydrate (Sigma-Aldrich, St. Louis, MO, USA), Ammonium Hydroxide (Sigma-Aldrich, St. Louis, MO, USA), Citrate Solution (Sigma-Aldrich, St. Louis, MO, USA)

Frequently Utilized Techniques

I. Washing/ Sterilization Methods for PPF scaffolds

A simple washing and sterilization technique was developed to ensure that the thin film coupons and 3D porous scaffolds were prepared for cell attachment. The washing was performed to clean the scaffolds from debris and remove any remaining uncured resin. The sterilization was performed to give a sterile environment for the cells. The wash and sterilization consisted of the following steps (Note: all PBS is at the 1X concentration):

<u>Wash</u>

1. Wash the PPF thin films with PBS for 5 minutes.
2. Aspirate the PBS, and replace with 70% acetone for 25 minutes.
3. Aspirate the 70% acetone and replace with PBS for 5 minutes. Perform two additional PBS washes for 5 minutes.
4. Aspirate the PBS, and replace with 70% acetone for 15 minutes.
5. Aspirate the 70% acetone and replace with PBS for 5 minutes. Perform two additional PBS washes for 5 minutes.
6. Aspirate the PBS, and replace with fresh PBS in preparation for the autoclave.

Sterilization

7. Autoclave on liquid cycle for sterilization.

8. Aspirate the PBS.

9. Place the PPF thin films in the well plate and incubate in FBS for 12 hours.

After completion of the wash, sterilization, and FBS incubation, the scaffolds are ready for cell seeding. The wash steps ensure there is no uncross-linked PPF on the thin film surface and FBS incubation ensures that the scaffolds will be best suited for cell attachment and proliferation.

II. Cell Culture

BM-hMSCs were obtained at passage # 3 (P3) from RoosterBio and were expanded using RoosterBio basal medium and were seeded at passage # 5 (P5) on 1x1 cm^2 PPF thin films. The cells were seeded by passage #5 to avoid the chance of any genetic drift or other variations which may occur at high passage numbers. The cells were seeded at a density of $2.5x10^4$ cells/cm^2. For the proliferation study, RoosterBio basal medium was supplemented with FGF, PDGF-BB and EGF at 1X concentration (5 ng/mL, 40 ng/mL and 20 ng/mL, respectively) or at 10X concentration (50 ng/mL, 400 ng/mL and 200 ng/mL, respectively). For differentiation, RoosterBio basal medium supplemented with the following osteogenic substances: dexamethasone (10^{-7}), β-glycerophosphate (10mM), and ascorbic acid (50 µg/ml) was additionally supplemented with BMP-4, BMP-6, or BMP-7 at 1X concentration (50 ng/ml, 50 ng/ml and 27 ng/ml, respectively) or at 10X concentration (500 ng/ml, 500 ng/ml, and 270 ng/ml, respectively). These values are tabulated with references in Table 1. The doses were chosen based on information in literature and cost.

III. MTT assay

MTT assay is used to determine cell proliferation quantitatively. A standard plot is first prepared so that absorbance values (A.U) can be correlated and the number of cells/group/time point can be determined. The thin films coated with cells for MTT assay were first washed in PBS. These were further incubated in 1 ml plain media containing 5 mg/ml MTT dye and incubated for 4 hours in CO_2 incubator under humidified (>95%) conditions in the presence 5% CO_2 at 37°C temperature. After incubation, the well plate was removed from the incubator and MTT reagent was aspirated out. To these well, 1 ml dimethyl sulfoxide (DMSO) was added to solubilize the formazan crystals. The purple color generated was read spectrophotometrically at 405 nm wavelength.

IV. SEM analysis

SEM imaging was performed for visualization of cell coating, distribution, and proliferation on the scaffold surface. The samples for SEM analysis were first washed in PBS and then fixed in 1% glutaraldehyde for 30 mins. Thereafter, these were treated with OsO_4 for enhancing the contrast of the fixed cells. Further, samples were sequentially treated with graded ethanol series from 50% to 100%. Samples were then dried in critical point dryer (Pelco) and followed by sputter coating in gold plasma (Cressington 108 Sputter coater). Once the samples were gold coated, they were viewed via scanning electron microscope (FEI Nova NanoSEM 400) under following settings: high voltage = 5kV, spot size = 3 and working distance = 6-7 mm.

V. Toluidine blue assay

Toluidine blue staining was used as a qualitative analysis method for cell proliferation. The main purpose was to confirm the trends observed during the MTT assay. Cells were washed in 1X PBS for 5 mins then fixed in 3.7% formaldehyde solution in 1X PBS for 10 mins at room

temperature. Samples were washed with PBS then 0.1% Triton X-100 in 1X PBS for 5 mins in humidified conditions. The samples were washed again in 1X PBS before being incubated in 1% Bovine Serum Albumin (BSA) for 30 mins at room temperature. The samples were then washed again for a final time in 1X PBS. A 1% Toluidine Blue and 1% sodium tetraborate solution was made in distilled water (w/v%). The solution was mixed using a magnetic stir rod and plate and filtered using filter paper and filter tip syringe. Once the solution was made, a few drops were added to the fixed cells in the well plate. The well plate was then placed into a 50°C oven until the stain began to dry in the well plate. Several rinses of distilled water was used to remove any solution from the sample. After distilled water washes, the samples were then rinsed first with 95% ethanol and then with 100% ethanol. The samples could be viewed either macroscopically or microscopically by qualitatively looking at the blue cells on the sample.

VI. Qualitative ALP Staining

Proliferating osteoblasts are known to produce alkaline phosphatase enzyme. As a result, these levels can be used to track the differentiation of hMSCs to osteoblasts and the proliferation of these osteoblasts. The ALP enzyme production of each of the groups was determined quantitatively by absorbance values at 405 nm. Qualitative ALP staining was performed to confirm results found in the ALP assay. The ALP staining samples were first fixed using a citrate buffered acetone solution. A diluted diazonium salt solution was created by dissolving a Fast Violet B capsule in distilled water. The alkaline dye solution was made by combining the dilute diazonium salt solution with Napthol AS-MX Phosphate Alkaline Solution (4% vol/vol). The samples were incubated in alkaline dye solution at room temperature for 30 minutes in the dark. Next, the samples were rinsed with deionized water for 2 min and then they were placed in Mayer's Hematoxylin Solution for 10 minutes. They were viewed microscopically.

VII. Quantitative ALP Assay

Quantitative ALP assay was performed to determine the relative amount of proliferating osteoblasts present on the scaffolds. One tablet of p-nitrophenol phosphate (pNPP) and one tablet of Tris buffer was dissolved in 20ml distilled water (20 ml). After the samples were incubated in alkaline phosphate stain, the stain was removed and the samples were washed thoroughly. pNPP substrate solution was added to each sample and they were incubated in the dark at room temperature for 30 minutes. After the incubation, the plate was read at 405 nm using a multi-well plate reader.

VIII. Alizarin Red S Staining

Alizarin Red S assay and staining can be used to determine bone mineralization because of the orange-red staining of calcium based mineral deposits/hydroxyapatite crystals. These crystal form as a result of osteoblastic activity during the later phase of osteoblast maturation. The media from the alizarin red S samples was removed and the samples were washed three times in 1X PBS. The cells were fixed using cold 70% ethanol for 1 hour and allowed to air dry. A 0.5% ammonium hydroxide solution was prepared by diluting a 30% stock ammonium hydroxide solution in distilled water. The 40mM alizarin red S staining solution was created by dissolving powdered alizarin red S in distilled water and the pH was adjusted to 4.1-4.3 using 0.5% ammonium hydroxide. The samples were stained using alizarin red S for 1 hour at room temperature. The samples were then rinsed three times with distilled water and were imaged microscopically.

IX. Alizarin Red S Assay

0.1M Sodium Phosphate buffer was made from stock solutions of 1M monobasic $NaH_2PO_4 \cdot H_2O$ and 1M dibasic Na_2HPO_4 in distilled water. 10% cetylpyridinium solution

(wt/vol) was made by dissolving solid cetylpyridinium in 0.1M Sodium Phosphate Buffer, pH 7.0. The alizarin red S staining samples were de-stained in 10% cetylpyridinium and the absorbance readings were collected at 562 nm using a multi-well plate reader.

Experiment Methods – Two Dimensional Study

I. Fabrication of Thin Film Two-Dimensional Scaffolds

PPF was synthesized in the laboratory of Dr. Matt Becker with financial support from an AFRIM grant (W81XWH-14-2-0004). 3:1 PPF:DEF resin was synthesized. The resin was then diluted 1:1 with diethyl fumarate (DEF) which is a dimer with a carbon to carbon double bond, so it can participate in the cross-linking network. Dissolving the PPF in DEF helps to reduce the viscosity of the resin so it can flow properly during 3D printing. The following photo-initiators and dyes were then added to the resin mixture to create an optimal photo-cross-linking environment: Irgacure 819/BAPO (0.7% w/w% with 1:1 PPF:DEF), Oxybenzone/2-Hydroxy-4-methoxybenzophenone (0.4% w/w%) and Irgacure 784 (0.3% w/w%). Once all photo-initiators and dyes were mixed adequately into the resin, thin films were cast by placing resin (~6-7 drops) in between two glass microscope slides. The slides were then placed into a UV box for 30 mins to promote enough cross-linking to cut the samples into 1x1 cm^2 squares. The samples were then placed back into the UV box for 7.5 hours to ensure all cross-linking has occurred. The structure of cross-linked PPF can be found in Figure 1. Once fully cross-linked, samples were washed and sterilized as described above.

II. Preliminary Study: Cytotoxicity

The cytotoxicity of the PPF thin films was analyzed using a live-dead assay in two ways: 1) by placing thin films on a BM-hMSC cell monolayer, and, 2) by seeding cells onto the thin films at a density of $2.5x10^4$ cells/cm^2. The cells in both the cases were first washed with PBS, thereafter,

live-dead stain was added at a concentration of 4 μM of calcein AM and 2 μM of ethidium homodimer (EthD) in PBS. These were incubated for 30 min at room temperature under dark conditions. After incubation, the live-dead stain was removed and ~ 20 μl PBS was added to each well in order to prevent drying during image procurement.

A cytotoxicity analysis with live-dead staining was performed to validate that the cured resin was biocompatible and suitable for cell proliferation and growth. Cells that were stained green were living and cells stained red were dead. Cells were seeded onto PPF scaffolds and observed using Bright field and fluorescence microscopy techniques. The microscopy images included in Figure 3 demonstrate viable cell attachment and growth which confirms the absence of cytotoxicity in the PPF scaffolds.

III. Preliminary Study: Cell Seeding Density

Prior to beginning the study, the cell seeding density was determined through a preliminary cell seeding density study. The study aimed to determine the best cell seeding density which uniformly coated the scaffold and allowed for cells to have adequate room for proliferation. Cell seeding density was determined by seeding cells at different densities onto PPF scaffolds and observing the cells under microscopy for uniform coating and low confluence. The cells were seeded at densities of 10,000, 25,000, 50,000, 100,000, and 200,000 cells/ml on thin films (n=3) in ultra-low attachment 24-well plates. The cells were incubated and allowed to attach for four hours. After the 4 hour incubation, bright field imaging was performed using Olympus CKX41 microscope (Olympus, Center Valley, PA) connected with a 12.8 MP digital camera.

IV. Growth Factor Literature Review for ECM Study

In order to determine the growth factors for proliferation and differentiation and respective doses, a literature review was undertaken. Previous work in the lab was referenced as well. After

careful review of the literature and previous work in the lab, we determined that FGF, PDGF, and EGF would be explored for their proliferation capabilities and that BMP-4, BMP-6, and BMP-7 would be explored for their differentiation capabilities. From the literature, the 1X doses were determined and tabulated in Table 1. The 10X dose was designed so that any potential difference between dose groups would be seen in the results if a difference existed.

Proliferation			
Growth Factor	1X Dose (ng/ml)	10X dose (ng/ml)	Reference
FGF-2	5	50	39
PDGF-BB	40	400	40
EGF	20	200	41
Differentiation			
Growth Factor	1X Dose (ng/ml)	10X dose (ng/ml)	Reference
BMP-4	50	500	28,33
BMP-6	50	500	33
BMP-7	27	270	42

Table 1: Growth factor dose (1X and 10X) for proliferation and differentiation factors. The doses were determined by references given.

V. Extracellular Matrix (ECM) Study

The ECM study was performed with the primary aim of achieving an ECM layer on PPF scaffolds. An ECM layer prior to implantation allows for the scaffold to mimic bone upon implantation into the patient. In order to achieve an ECM layer, four experimental groups were studied for the analysis of cell proliferation, i.e., 1) 1X dose of FGF-2, PDGF-BB, EGF (E1X), 2) 10X dose of FGF-2, PDGF-BB, EGF (E10X), 1X dose of FGF-2, PDGF-BB (NE1X), and, 10X dose of FGF-2 and PDGF-BB (NE10X) in hMSC Differentiation Basal Medium from RoosterBio Inc. Here, 'E' stands for group containing EGF, and, 'NE' stands for the group not containing any EGF. The control media (CM) group for cell proliferation was hMSC Differentiation Basal Medium from RoosterBio Inc. that did not contain any growth factors.

Seven experimental groups were studied for cell differentiation, i.e., OM (osteogenic media containing 10^{-7} M dexamethasone, 10 mM β-glycerophosphate and 50 μg/ml ascorbic acid), 1X

and 10X BMP-4 (1X and 10X dose of BMP-4 in osteogenic media), 1X and 10X BMP-6 (1X and 10X dose of BMP-6 in osteogenic media), 1X and 10X BMP-7 (1X and 10X dose of BMP-7 in osteogenic media). The control group for differentiation study was the same as proliferation study. A schematic of the general work flow can be found in Figure 2.

Experiment Methods – Three-Dimensional Study

I. Fabrication of Three-Dimensional Porous Scaffolds

The same resin chemistry as the 2D thin film scaffolds was used to print 3D cylindrical scaffolds of 6 mm diameter and 5 mm height with Schoen's gyroid pore geometry. Other features include the strut size of 187.5 µm, pore size of 625 µm, surface area of 342.27 mm^2 and volume of 17.77 mm^3. A computer aided design (CAD) file of these features was created using SolidWorks software (Dassault Systèmes, Waltham, MA). Further, this CAD file was 3D printed by using an EnvisionTEC Perfactory P3 3D printer (Dearborn, MI). To remove the cytotoxic uncured resin from the cross-linked polymer, washing was performed using 70% acetone and PBS. The samples were then sterilized in an autoclave and FBS incubated overnight before cell seeding.

II. Replication of Two-Dimensional Findings on Three-Dimensional Scaffolds

In order to show a smooth translation from 2D to 3D scaffolds, a 1X dose of EGF, FGF, and PDGF, as determined by the 2D study, was used to proliferate cells on the 3D porous scaffolds. The proliferation and coating will be observed by using SEM analysis at day 0 and day 7. Later, the full 2D study will be completed on the 3D scaffolds to show complete translation of the results. The study was attempted, but contamination led to poor results. The study will be repeated.

Results and Discussions – Two Dimensional Study

Determination of Cell Seeding Density

Cell seeding density was determined by seeding different densities of cells onto PPF thin film scaffolds and observing the cells under a microscope for cell coating and optimal density. After comparing the various cell seeding densities, it was determined that a cell seeding density of 25,000 cells/ml was sufficient for uniform coating and produced a low density cell coat. A low density cell coating was desirable in order to limit cell usage and allow for proliferation of cells over time. In Figure 3, it is clear that 10,000 cells/ml (Figure 3A) did not produce a uniform cell coating and cell seeding densities of 50,000 cells/ml or higher (Figure 3C-E) led to high cell densities which would limit cell proliferation capabilities. Therefore, 25,000 cells/ml (Figure 3B) was used for the experiments.

Analysis of Cell Proliferation

I. MTT Assay

As observed in Figure 4A, all groups show an increasing trend from day 1 to day 7. At day 7, the values of cell number for NE1X, NE10X, E1X, E10X, and, CM groups were 91705.93±11965.23, 110208.75±4902.20, 116023.73±5164.69, 102212.32±16281.94 and, 36976.08±4490.06, respectively. Among the groups of defined factors, E1X showed significantly higher proliferation than the NE1X and CM groups ($p=0.001$ and $p=0.000$, respectively). NE1X also showed significantly higher cell proliferation than the CM group ($p=0.000$). A similar trend was observed at the 10X dosage as well. However, there was not a significant difference between the results for the 1X and 10X doses. Therefore, it was determined that the 1X dosage would be appropriate and more cost effective for achieving cell proliferation on the thin film scaffolds.

II. Toluidine Blue Staining

In Figure 4B, the cells represented by blue color show an increasing trend from day 1 to day 7 for all groups. The CM (control) group showed very little proliferation between day 1 and day 7. The CM group did not have any growth factors added. The rest of the groups which contained growth factors, such as E1X, E10X, NE1X, and NE10X, showed much higher cell proliferation than the CM group. These results for cell proliferation, therefore, follow the trend observed in the MTT assay.

III. SEM imaging and analysis

Figure 5A shows that at day 0, the cell distribution was uniform on the surface of the thin film coupons for all growth factor groups. Based on visual observation of the cells at this time point, it was determined that round morphology of the cells suggested initial attachment. By day 7 in Figure 5B, all of the groups showed uniform cell spreading, coating, and distribution. At this time point, it appeared that the thin film scaffolds were completely coated with cells. Therefore, we chose the day 7 time point for switching the environment of the cells to osteogenic media for osteogenic differentiation. It is important to note the difference in appearance of the cells from growth factor containing groups and the CM (control) group. The CM group showed better cell spreading at both day 0 and day 7. Perhaps there is a difference of cell behavior in the presence of growth factors.

Analysis of hMSC differentiation

I. Alkaline Phosphatase Assay and Stain

In Figure 6A, all groups show an increasing trend from MSC to osteoblast from day 14 to day 21 (day 0 to day 7 is cell proliferation). The average values at day 14 for BMP-4 1X, BMP-4 10X, BMP-6 1X, BMP-6 10X, BMP-7 1X, BMP-7 10X, OM and CM are 2.52±0.51, 3.23±0.10,

2.80±0.25, 3.22±0.11, 2.54±0.43, 1.45±0.34, 3.28±0.14, 0.76±0.30 A.U., respectively. While, the readings for the same sequence of groups at day 21 was as follows: 6.11±0.18, 6.49±0.10, 6.50±0.09, 6.45±0.11, 5.96±0.19, 6.54±0.09, 6.39±0.11, 1.23±0.11 A.U., respectively. Statistical analysis at day 14 showed that the osteogenic media showed significantly higher values than any of than 1X doses of BMP-4 ($p=.000$), BMP-6 ($p=.010$) and BMP-7 ($p=.000$), along with, BMP-7 10X ($p=.000$) and CM ($p=.000$). However, analysis at day 21 shows that osteogenic media only has significantly higher values than BMP-7 1X ($p=.006$) and CM ($p=0.000$). Additionally, the 10X doses were found to be significantly higher ($p<0.05$) for all of the groups except for the BMP-6 group at day 21.

ALP Staining was performed to qualitatively confirm the trends observed in the ALP assay. The red color in and around the cells indicates the presence of ALP enzyme. As shown in Figure 6B, an increasing trend was observed from day 14 to day 21 for all of the groups. This observation matches the results found in the quantitative ALP assay.

II. Alizarin Red S Assay and Stain for Bone Mineralization

Figure 7A shows an increasing trend for bone mineralization for all growth factor groups from day 14 to day 21. The average values at day 14 for BMP-4 1X, BMP-4 10X, BMP-6 1X, BMP-6 10X, BMP-7 1X, BMP-7 10X, OM and CM are 0.30±0.04, 0.35±0.04, 0.30±0.03, 0.31±0.05, 0.36±0.06, 0.31±0.04, 0.25±0.02, 0.21±0.02 A.U., respectively. While, the readings for the same sequence of groups at day 21 was as follows: 0.37±0.06, 0.45±0.05, 0.49±0.06, 0.53±0.04, 0.79±0.07, 0.75±0.05, 0.41±0.06, 0.26±0.05 A.U., respectively. In Figure 7A, the BMP-7 group showed a significantly higher level of mineralization at day 21 than all other groups ($p<0.000$), regardless of concentration. Also, it was found that BMP 7 1X and 10X did not differ much in effectiveness. Therefore, it was found that the BMP-7 1X dose would be sufficient and most cost

effective for inducing mineralization of osteoblastic cells formed during osteogenic differentiation of hMSCs on PPF polymer surfaces. These results were further confirmed by the observation of similar trends during the qualitative analysis of alizarin red S staining shown in Figure 6B.

III. SEM Analysis for Cell Differentiation

SEM imaging and analysis was performed at day 21 for each group in order to visualize the mineralized crystal formation on the PPF thin film scaffolds. The images can be found in Figure 8. The images for each group showed formation of crystal like structures represented by whitish dots on cell layers suggesting mineralization of the osteoblast. All of the groups showed uniform distribution of crystals, except the CM group. The observed crystals are closely linked with ECM thread, which further suggests the presence of hydroxyapatite crystals formed at the nucleation sites of collagenous matrix typically found during osteogenic maturation and mineralization of osteoblasts.

Results and Discussions - Three-Dimensional Study

Analysis of hMSC Proliferation and Coating

I. SEM Analysis for Cell Proliferation and Coating

A critical step for our research efforts is to validate the feasibility of the translation of results obtained from 2D thin film surface studies to 3D printed scaffolds. The first step for assessing the feasibility is the uniform seeding of cells on the 3D scaffold surface along with proliferation of those cells at a later time point. Therefore, we assessed this phenomenon via SEM analysis at day 0 and day 7 (Fig. 8). As shown in Fig. 8A and B, at day 0, the BM-hMSCs initially show a rounded morphology with initiation of spreading at some places. Whereas, at later time point of day 7, all the cells show spreading on the scaffold surface as observed in Fig. 8C and D.

Final Conclusions

The present study provides an optimized regimen of growth factors for the proliferation and differentiation of BM-hMSCs on the surface of 2D and 3D PPF scaffolds. It suggests the suitability of PPF polymer for the development of artificial bone tissue engineered biomaterials containing a layer of extracellular matrix on their surface for the treatment of bone defects. Achieving an ECM layer on the surface of the scaffolds is important for the preparation of the bone graft prior to implantation.

Future Work

Three-Dimensional Study

Further work will need to be completed for the three-dimensional study. Although cell proliferation and coating was achieved on the 3D polymer scaffold, as shown in Figure 9A-D, a complete duplicate study modeling the two-dimensional study will need completed to confirm our results quantitatively. A study was previously attempted but contamination issues led to poor data and bad results. Therefore, redoing the study will be a must for our future work.

Defined Media Study

The defined media study was begun to ensure that our defined media and growth factor doses were as efficient and effective as undefined, commercial media in producing BM-hMSC proliferation and differentiation to osteoblast. The main purpose for having a defined media is for future aspirations of clinical trials in which defined components will be necessary for receiving permission to perform the trial. For this study, RoosterBio media with osteogenic factors of dexamethasone (10^{-7}), β-glycerophosphate (10mM), and ascorbic acid (50 µg/ml) along with defined growth factors were evaluated for osteogenic differentiation. The defined growth factors for proliferation as determined by the present study are the following: FGF (5

ng/ml), PDGF-b (40 ng/ml), and EGF (20 ng/ml). The defined growth factor added for differentiation is BMP-7 (27 ng/ml). These proliferation and differentiation media will be compared to Lonza proliferation and osteogenic differentiation media and OH-Alive 4 step media system for osteogenic differentiation. In order to test the different media, cells will be seeded on 2D thin film coupons as determined by the present study. The study will be run for one week in proliferation media in accordance with our 2D thin film results. Some samples will be pulled to study the efficiency of the media to facilitate cell proliferation by using MTT, SEM, and Toluidine Blue. The culturing environment will then be changed to differentiation media suitable for cell differentiation into osteoblast for the remaining samples and the study is concluded at two weeks, i.e. 14 days. The differentiation and mineralization of the cells will be analyzed by ALP stain and assay and Alizarin Red S stain and assay. SEM images will also be taken again for additional qualitative assessment. The results for each media type will be compared to each other to determine the effectiveness of each media type for the desired proliferation and differentiation of the cells.

Other Work

As a result of our findings on 2D thin film coupons and 3D porous, cylindrical scaffolds, it would be appropriate and interesting to continue research in bioactive molecules as well as seeding methods for scaffolds of different sizes and shapes. Future work will look to develop seeding methods and defined factors which can be repeated on scaffolds for patient-specific implants. This will be achieved by reproducing 3D study findings on 3D scaffolds of various shapes. It is extremely important to have a defined method since areas of trauma will be variable amongst patients. Also, the incorporation of ligands (as bioactive molecules) with the surface of the polymer will be explored regarding cell attachment, proliferation, and differentiation.

In addition, several animal studies will be completed to advance our work towards clinical trials. Animal models will include mice, rats, and larger animals such as dogs. Previously, a SCID mouse study was completed to show vascularization could be achieved through the pores of the scaffold. Results showed that vascularization could be achieved on scaffolds, imbedded with novel spheroids of HUVECs and HMSCs, implanted subcutaneously. Although this work is not presented in this document, it contributes to our desires to pursue other animal studies. One possible study will involve implanting 3D porous scaffolds into rats for the purpose of repairing segmental femur defects. Another potential future study is a dog mandible study. In such a study, a PPF mandibular implant will be pre-seeded using in-house techniques that produce proliferating osteoblasts prior to implantation, with the direction that the cells will further mature into bone. These animal model studies, hopefully, will aid in our pursuit to gain approval for a human clinical study in the future. The aim is to provide a defined, repeatable method for developing successful, patient specific bone grafts which perform with less limitations than traditional bone grafts.

Acknowledgments

I would like to thank the Osteo Engineering Lab (laboratory of David Dean, PhD) in the Department of Plastic Surgery for their continued support and funding for my research endeavors. I would like to thank Ruchi Mishra, PhD for her training and continued help and guidance throughout my time in the lab. I would also like to thank Tyler Bishop, Stefani Montelone, and Briana Swan for the help in completing the projects. Lastly, I would like to thank the Undergraduate Education Research Fellowship, College of Arts and Sciences for research support through a stipend.

This work was supported by the Army, Navy, NIH, Air Force, VA and Health Affairs to support the AFIRM II, under Award No. W81XWH-14-2-0004.

References

1. Leventhal, G. S. (1951). Titanium, a metal for surgery. *The Journal of Bone & Joint Surgery*, *33*(2), 473-474.
2. Burke, G. L. (1940). The corrosion of metals in tissues; and an introduction to tantalum. *Canadian Medical Association Journal*, *43*(2), 125.
3. Olmedo, D. G., Duffó, G., Cabrini, R. L., & Guglielmotti, M. B. (2008). Local effect of titanium implant corrosion: an experimental study in rats.*International journal of oral and maxillofacial surgery*, *37*(11), 1032-1038.
4. Noyama, Y., Miura, T., Ishimoto, T., Itaya, T., Niinomi, M., & Nakano, T. (2012). Bone loss and reduced bone quality of the human femur after total hip arthroplasty under stress-shielding effects by titanium-based implant.*Materials Transactions*, *53*(3), 565-570.
5. Nagels, J., Stokdijk, M., & Rozing, P. M. (2003). Stress shielding and bone resorption in shoulder arthroplasty. *Journal of Shoulder and Elbow Surgery*,*12*(1), 35-39.
6. Mistry, A. S., & Mikos, A. G. (2005). Tissue engineering strategies for bone regeneration. In *Regenerative medicine II* (pp. 1-22). Springer Berlin Heidelberg.
7. Bose, S., Roy, M., & Bandyopadhyay, A. (2012). Recent advances in bone tissue engineering scaffolds. *Trends in biotechnology*, *30*(10), 546-554.
8. Gerhardt, L. C., & Boccaccini, A. R. (2010). Bioactive glass and glass-ceramic scaffolds for bone tissue engineering. *Materials*, *3*(7), 3867-3910.

9. Rezwan, K., Chen, Q. Z., Blaker, J. J., & Boccaccini, A. R. (2006). Biodegradable and bioactive porous polymer/inorganic composite scaffolds for bone tissue engineering. *Biomaterials*, *27*(18), 3413-3431.
10. Dean, D., Topham, N. S., Meneghetti, S. C., Wolfe, M. S., Jepsen, K., He, S., ... & Mikos, A. G. (2003). Poly (propylene fumarate) and poly (DL-lactic-co-glycolic acid) as scaffold materials for solid and foam-coated composite tissue-engineered constructs for cranial reconstruction. *Tissue engineering*,*9*(3), 495-504.
11. Dean, D., Wallace, J., Siblani, A., Wang, M. O., Kim, K., Mikos, A. G., & Fisher, J. P. (2012). Continuous digital light processing (cDLP): Highly accurate additive manufacturing of tissue engineered bone scaffolds: This paper highlights the main issues regarding the application of Continuous Digital Light Processing (cDLP) for the production of highly accurate PPF scaffolds with layers as thin as 60 μm for bone tissue engineering. Virtual and physical prototyping, 7(1), 13-24.
12. Dean, D., Mott, E., Luo, X., Busso, M., Wang, M. O., Vorwald, C., ... & Fisher, J. P. (2014). Multiple initiators and dyes for continuous Digital Light Processing (cDLP) additive manufacture of resorbable bone tissue engineering scaffolds: A new method and new material to fabricate resorbable scaffold for bone tissue engineering via continuous Digital Light Processing. *Virtual and Physical Prototyping*, *9*(1), 3-9.
13. Fisher, J. P., Dean, D., & Mikos, A. G. (2002). Photocrosslinking characteristics and mechanical properties of diethyl fumarate/poly (propylene fumarate) biomaterials. *Biomaterials*, *23*(22), 4333-4343.

14. Kim, K., Yeatts, A., Dean, D., & Fisher, J. P. (2010). Stereolithographic bone scaffold design parameters: osteogenic differentiation and signal expression.*Tissue Engineering Part B: Reviews*, *16*(5), 523-539.
15. Wallace, J., Wang, M. O., Thompson, P., Busso, M., Belle, V., Mammoser, N., ... & Welter, J. F. (2014). Validating continuous digital light processing (cDLP) additive manufacturing accuracy and tissue engineering utility of a dye-initiator package. *Biofabrication*, *6*(1), 015003.
16. Wang, M. O., Vorwald, C. E., Dreher, M. L., Mott, E. J., Cheng, M. H., Cinar, A., ... & Fisher, J. P. (2015). Evaluating 3D-Printed Biomaterials as Scaffolds for Vascularized Bone Tissue Engineering. *Advanced Materials*, *27*(1), 138-144.
17. Cooke, M. N., Fisher, J. P., Dean, D., Rimnac, C., & Mikos, A. G. (2003). Use of stereolithography to manufacture critical-sized 3D biodegradable scaffolds for bone ingrowth. *Journal of Biomedical Materials Research Part B: Applied Biomaterials*, *64*(2), 65-69.
18. Wang, M. O., Etheridge, J. M., Thompson, J. A., Vorwald, C. E., Dean, D., & Fisher, J. P. (2013). Evaluation of the in vitro cytotoxicity of cross-linked biomaterials. Biomacromolecules, 14(5), 1321-1329.
19. Caplan, A. I. (2009). Why are MSCs therapeutic? New data: new insight. The Journal of pathology, 217(2), 318-324.
20. Murphy, M. B., Moncivais, K., & Caplan, A. I. (2013). Mesenchymal stem cells: environmentally responsive therapeutics for regenerative medicine. Experimental & molecular medicine, 45(11), e54.

21. Le Blanc, K., & Ringdén, O. (2005). Immunobiology of human mesenchymal stem cells and future use in hematopoietic stem cell transplantation. Biology of Blood and Marrow Transplantation, 11(5), 321-334.
22. Abdi, R., Fiorina, P., Adra, C. N., Atkinson, M., & Sayegh, M. H. (2008). Immunomodulation by mesenchymal stem cells a potential therapeutic strategy for type 1 diabetes. Diabetes, 57(7), 1759-1767.
23. Bueno, E. M., & Glowacki, J. (2011). Biologic foundations for skeletal tissue engineering. Synthesis Lectures on Tissue Engineering, 3(1), 1-220.
24. Eom, Y. W., Oh, J. E., Lee, J. I., Baik, S. K., Rhee, K. J., Shin, H. C., ... & Shim, K. Y. (2014). The role of growth factors in maintenance of stemness in bone marrow-derived mesenchymal stem cells. Biochemical and biophysical research communications, 445(1), 16-22.
25. Gharibi, B., & Hughes, F. J. (2012). Effects of medium supplements on proliferation, differentiation potential, and in vitro expansion of mesenchymal stem cells. *Stem cells translational medicine*, sctm-2010.
26. Auletta, J. J., Zale, E. A., Welter, J. F., & Solchaga, L. A. (2011). Fibroblast growth factor-2 enhances expansion of human bone marrow-derived mesenchymal stromal cells without diminishing their immunosuppressive potential. *Stem cells international*, *2011*.
27. Kondo, A., Tokuda, H., Matsushima-Nishiwaki, R., Kuroyanagi, G., Yamamoto, N., Mizutani, J., ... & Otsuka, T. (2014). Rho-kinase limits BMP-4-stimulated osteocalcin synthesis in osteoblasts: regulation of the p38 MAP kinase pathway. *Life sciences*, *96*(1), 18-25

28. Park, K. H., Han, D. I., Rhee, Y. H., Jeong, S. J., Kim, S. H., & Park, Y. G. (2010). Protein kinase C βII and δ/θ play critical roles in bone morphogenic protein-4-stimulated osteoblastic differentiation of MC3T3-E1 cells.*Biochemical and biophysical research communications*, *403*(1), 7-12.
29. Burkus, J. K., Heim, S. E., Gornet, M. F., & Zdeblick, T. A. (2003). Is INFUSE bone graft superior to autograft bone? An integrated analysis of clinical trials using the LT-CAGE lumbar tapered fusion device. *Journal of spinal disorders & techniques*, *16*(2), 113-122.
30. De Biase, P., & Capanna, R. (2005). Clinical applications of BMPs. *Injury*,*36*(3), S43-S46.
31. Park, J. S., Yang, H. N., Jeon, S. Y., Woo, D. G., Na, K., & Park, K. H. (2010). Osteogenic differentiation of human mesenchymal stem cells using RGD-modified BMP-2 coated microspheres. *Biomaterials*, *31*(24), 6239-6248.
32. Honda, Y., Ding, X., Mussano, F., Wiberg, A., Ho, C. M., & Nishimura, I. (2013). Guiding the osteogenic fate of mouse and human mesenchymal stem cells through feedback system control. *Scientific reports*, *3*.
33. Sammons, J., Ahmed, N., El-Sheemy, M., & Hassan, H. T. (2004). The role of BMP-6, IL-6, and BMP-4 in mesenchymal stem cell-dependent bone development: effects on osteoblastic differentiation induced by parathyroid hormone and vitamin D3. *Stem cells and development*, *13*(3), 273-280.
34. Shen, B., Wei, A., Whittaker, S., Williams, L. A., Tao, H., Ma, D. D., & Diwan, A. D. (2010). The role of BMP-7 in chondrogenic and osteogenic differentiation of human bone

marrow multipotent mesenchymal stromal cells in vitro. *Journal of cellular biochemistry*, *109*(2), 406-416.

35. Eap, S., Keller, L., Schiavi, J., Huck, O., Jacomine, L., Fioretti, F., ... & Benkirane-Jessel, N. (2015). A living thick nanofibrous implant bifunctionalized with active growth factor and stem cells for bone regeneration. *International journal of nanomedicine*, *10*, 1061.
36. Kanakaris, N. K., Calori, G. M., Verdonk, R., Burssens, P., De Biase, P., Capanna, R., ... & Kontakis, G. (2008). Application of BMP-7 to tibial non-unions: a 3-year multicenter experience. *Injury*, *39*, S83-S90.
37. Epstein, N. (2013). Complications due to the use of BMP/INFUSE in spine surgery: the evidence continues to mount. *Surgical neurology international*,*4*, 343.
38. Benglis, D., Wang, M. Y., & Levi, A. D. (2008). A comprehensive review of the safety profile of bone morphogenetic protein in spine surgery. Neurosurgery, 62(5), ONS423-ONS431.
39. Ahn, H. J., Lee, W. J., Kwack, K., & Kwon, Y. D. (2009). FGF2 stimulates the proliferation of human mesenchymal stem cells through the transient activation of JNK signaling. FEBS letters, 583(17), 2922-2926.
40. Jin, Y., Zhang, W., Liu, Y., Zhang, M., Xu, L., Wu, Q., ... & Jiang, X. (2014). Rhpdgf-bb via erk pathway osteogenesis and adipogenesis balancing in adscs for critical-sized calvarial defect repair. Tissue Engineering Part A, 20(23-24), 3303-3313.
41. Fekete, N., Rojewski, M. T., Lotfi, R., & Schrezenmeier, H. (2013). Essential components for ex vivo proliferation of mesenchymal stromal cells. Tissue Engineering Part C: Methods, 20(2), 129-139.

42. Jia, C., Liu, H., Li, M., Wu, Z., & Feng, X. (2014). Effects of icariin on cytokine-induced ankylosing spondylitis with fibroblastic osteogenesis and its molecular mechanism. *International journal of clinical and experimental pathology*, *7*(12), 9104.

43. Bohner, M. (2010). Resorbable biomaterials as bone graft substitutes. Materials Today, 13(1), 24-30.

44. Albrektsson, T., Brånemark, P. I., Hansson, H. A., & Lindström, J. (1981). Osseointegrated titanium implants: requirements for ensuring a long-lasting, direct bone-to-implant anchorage in man. Acta Orthopaedica Scandinavica, 52(2), 155-170.

45. Parikh, S. N. (2002). Bone graft substitutes: past, present, future. *Journal of postgraduate medicine*, *48*(2), 142.

Figures for Growth Factors dose determination and 2D to 3D sample translation for PPF Tissue Engineered Bone Implants

By

Ryan Sefcik

The Ohio State University

April 2016

Project Advisor: Dr. David Dean Ph.D., Department of Plastic Surgery

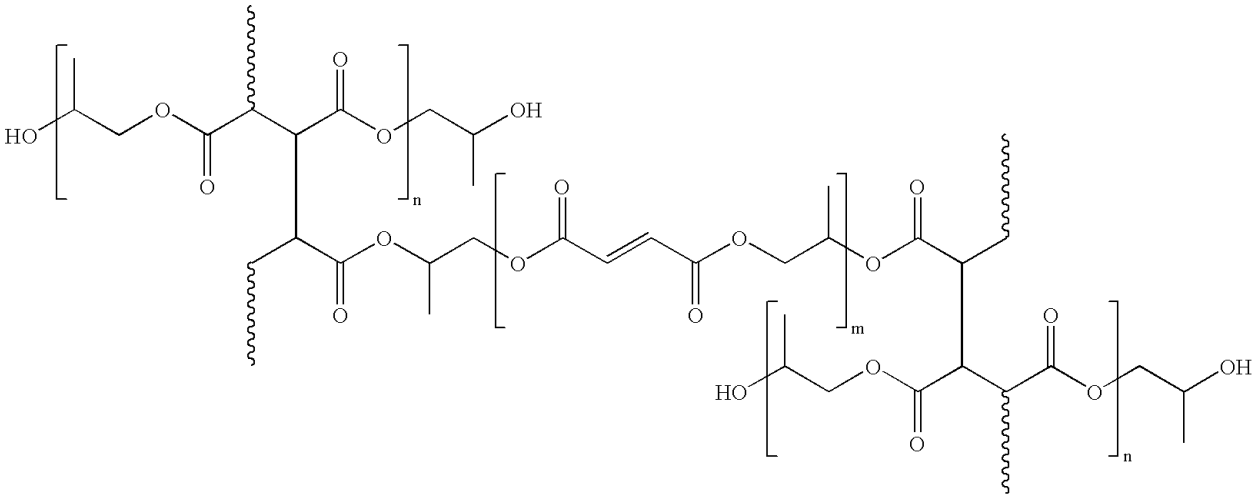

Figure 1. Photo-crosslinked PPF through the carbon to carbon double bond. The repeating unit can be found in the brackets.

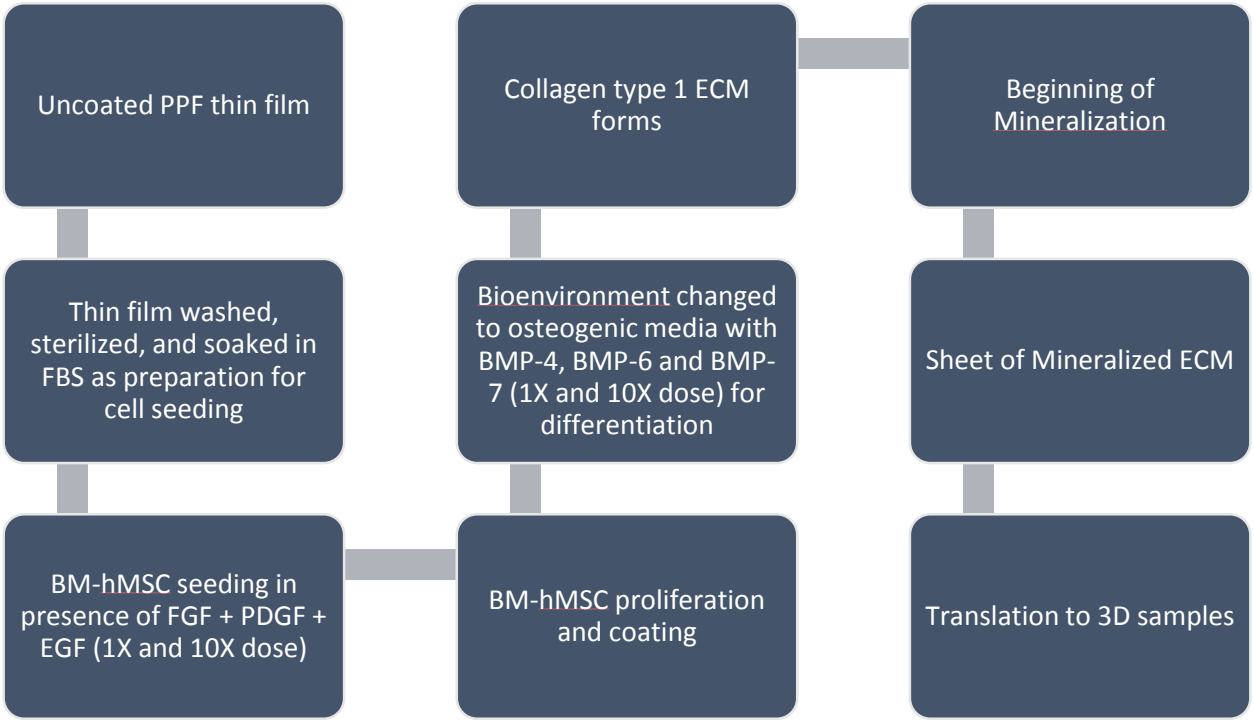

Figure 2. A schematic representation of the experiment plan for the ECM study for the 2D ECM study. Finally, the translation ECM layer deposition from 2D thin films to 3D printed scaffolds with gyroid pore geometry having open pore structure is shown as the final step for preparation of artificial PPF polymer based bone tissue engineered grafts.

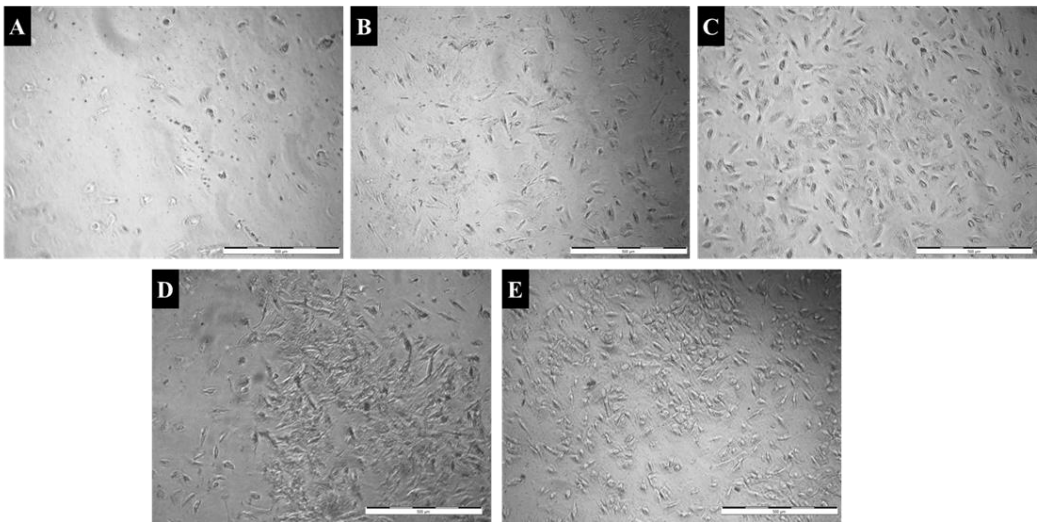

Figure 3. Determination of optimum cell seeding density for the study of BM-hMSC proliferation on PPF polymer surface. The bright field microscope images of BM-hMSC seeded PPF thin films are shown at cell densities of 10,000, 25,000, 50,000, 100,000, and, 200,000 cells/ml (A through D, respectively). The density of 25,000 cells/ml was chosen as initial cell density due to uniform and scattered distribution of cells (scale bar = 500μm). Additionally, 25,000 cells will allow for the proliferation of cells.

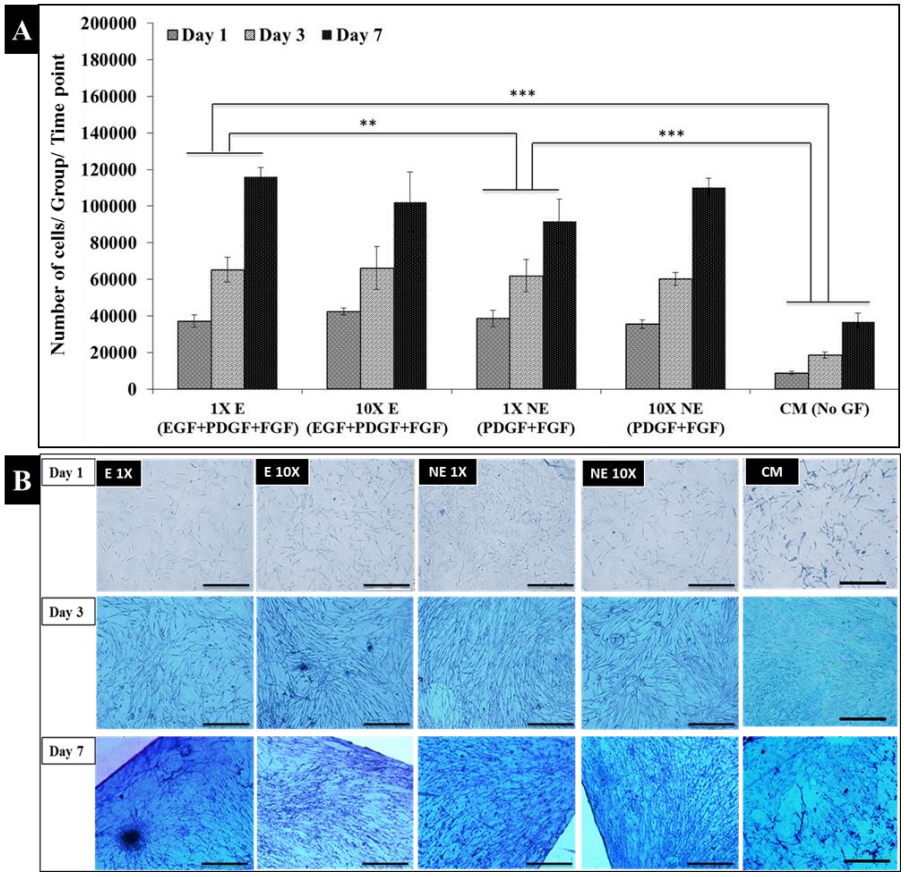

Figure 4. Study of cell proliferation in the presence of FGF-2, EGF and PDGF growth factors at 1X and 10X doses. In 4A, the cell number determined by MTT assay shows a significantly (p**=0.001) higher cell proliferation in 1X EGF containing (E1X) group in comparison to the group without EGF (NE1X). Whereas, the control media (CM) depicts lowest cell proliferation. Figure 4B represents the qualitative analysis of these results through toluidine blue staining. All the groups show increasing trend of cell proliferation from day 1 and day 7 similar to that of MTT results (scale bar = 500µm). This confirms the results of the MTT assay qualitatively.

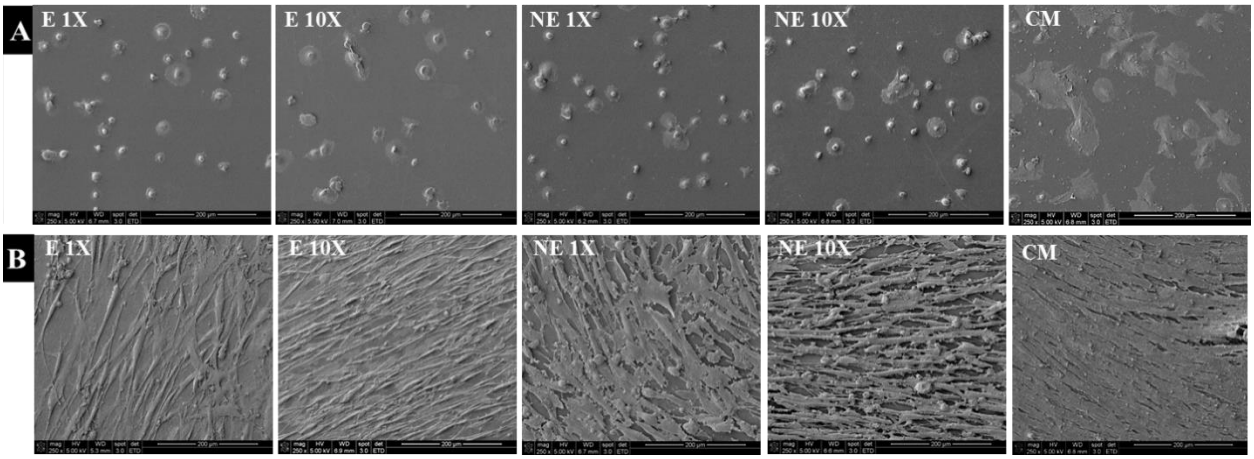

Figure 5. Scanning electron microscope image analysis of BM-hMSC proliferation. As shown in 5A, all the growth factor containing groups (E1X, NE1X, E10X and NE10X) show similar initial attachment at day 0 with mostly rounded morphology. While, these cells spread uniformly and coat the polymer surface by day 7 as demonstrated in 5B. However, the CM group shows higher cell spreading at both the time points (magnification of all images = 250X).

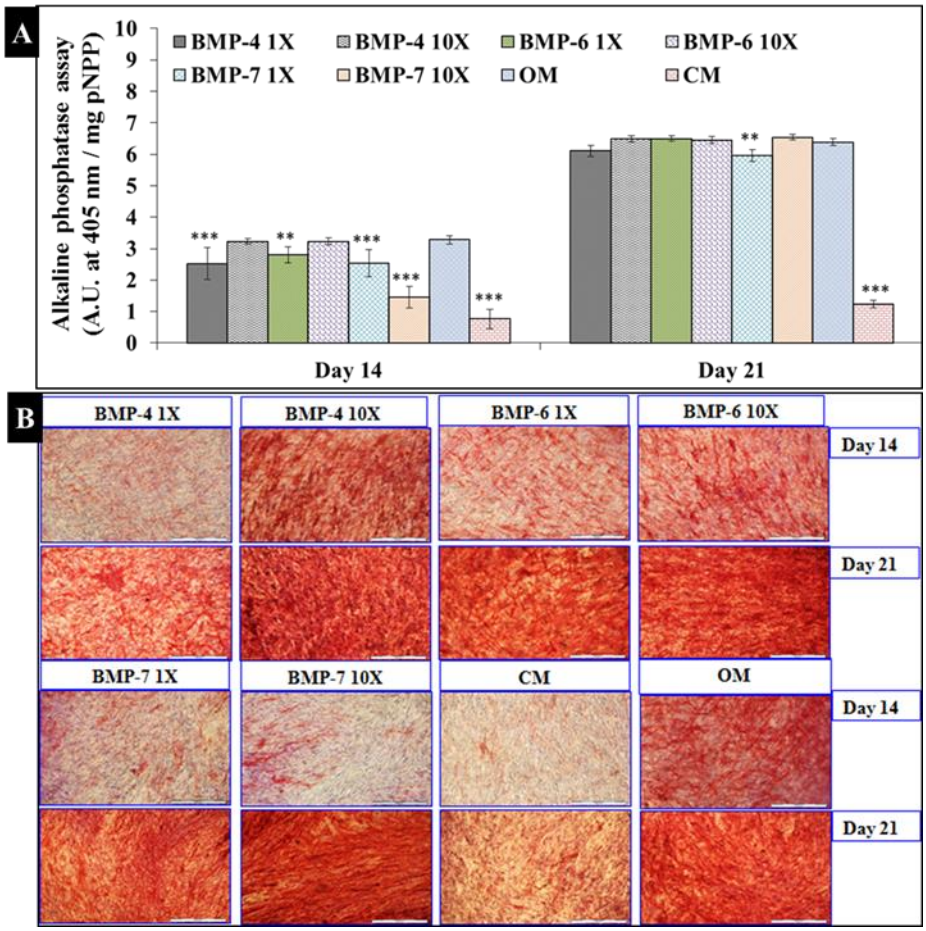

Figure 6. Analysis of osteogenic differentiation through alkaline phosphatase (ALP) enzyme assay and staining. During ALP enzyme assay, shown in 6A, all the groups show increase in absorbance readings with increase in time day 14 to 21. OM group at day 14 time point shows significantly ($p^{*}\leq0.05$, $p^{**}\leq0.01$, $p^{***}\leq0.001$) higher values than all other groups except BMP-4 10X and BMP-6 10X. While, at day 21, growth factor containing groups show a rapid increase in ALP production and OM group only shows statistically higher values than BMP-7 1X ($p^{**}\leq0.01$) and CM group ($p^{***}\leq0.001$). 6B depicts the ALP staining results for the same group types and the diffused red staining indicated the presence of enzyme. All the groups showed results similar to that of ALP assay during staining (scale bar = 500μm).

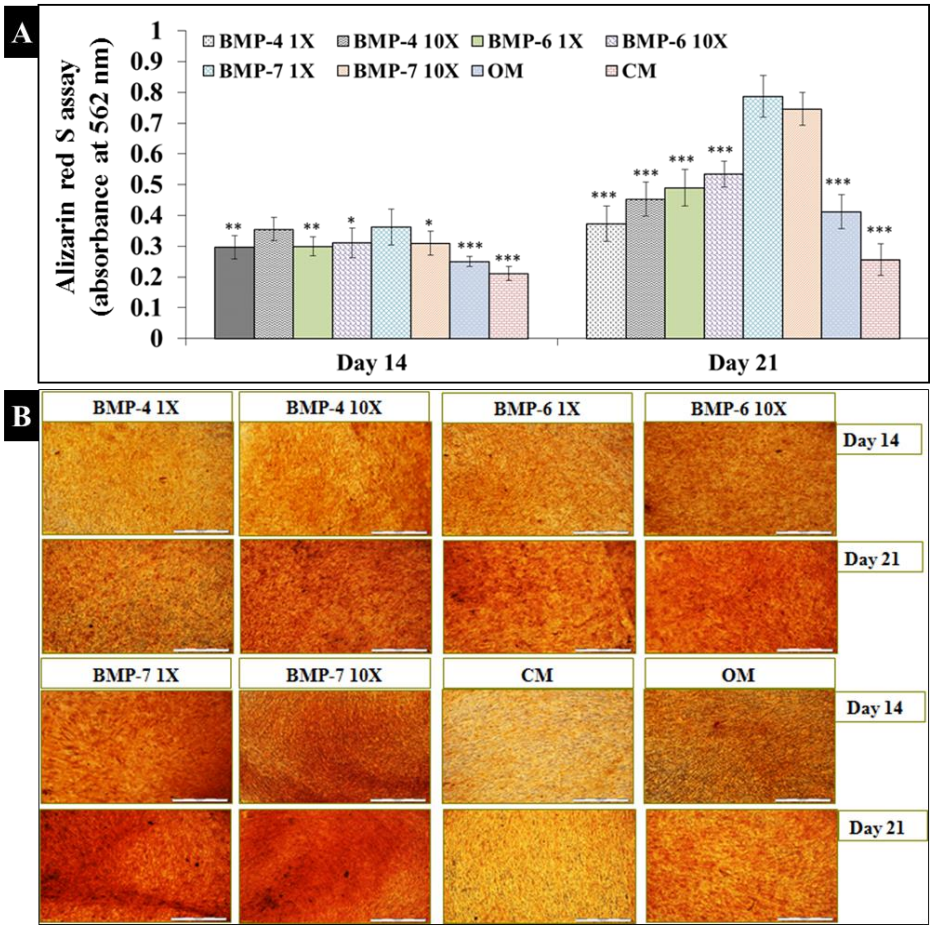

Figure 7. Study of osteogenic mineralization through alizarin red S assay and staining. As shown in 7A, BMP-7 1X group shows significantly ($p^{*}\leq0.05$, $p^{**}\leq0.01$, $p^{***}\leq0.001$) higher mineralization than all the other groups except BMP-4 10X group at day 14 time point. Whereas at day 21 BMP-7 (1X and 10X) group displays significantly higher mineralization than all other groups. As observed in 7B, similar results were obtained during the staining studies for mineralization represented by orange-red color staining at the mineralized areas (scale = 500μm).

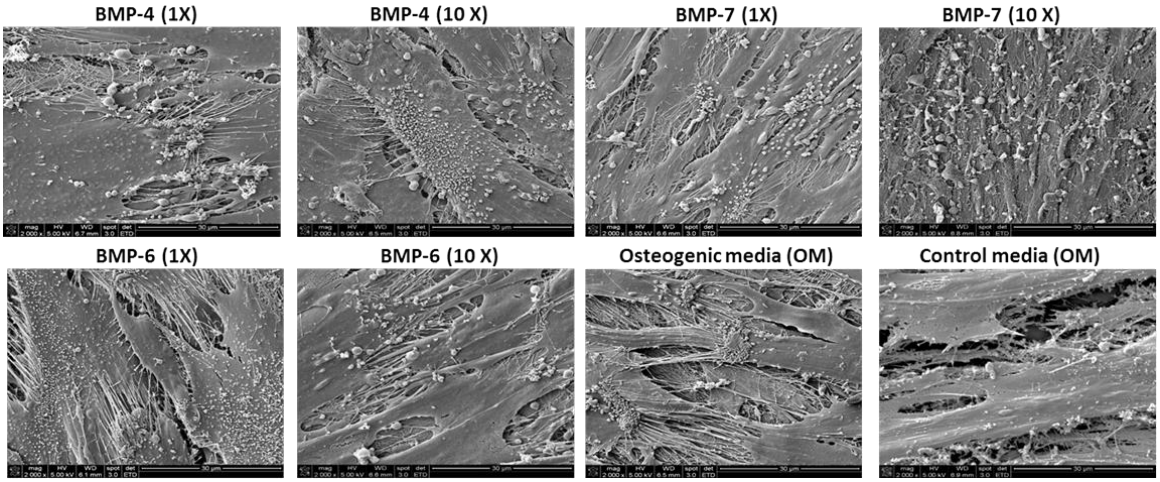

Figure 8. Scanning electron microscopy image analysis of mineralization. All the groups (except control) show extensive mineralization via presence of depicted hydroxyapatite-like crystals depicted by whitish dots associated with extracellular matrix threads. As expected, the CM group shows least mineralization (magnification of all images = 2000X).

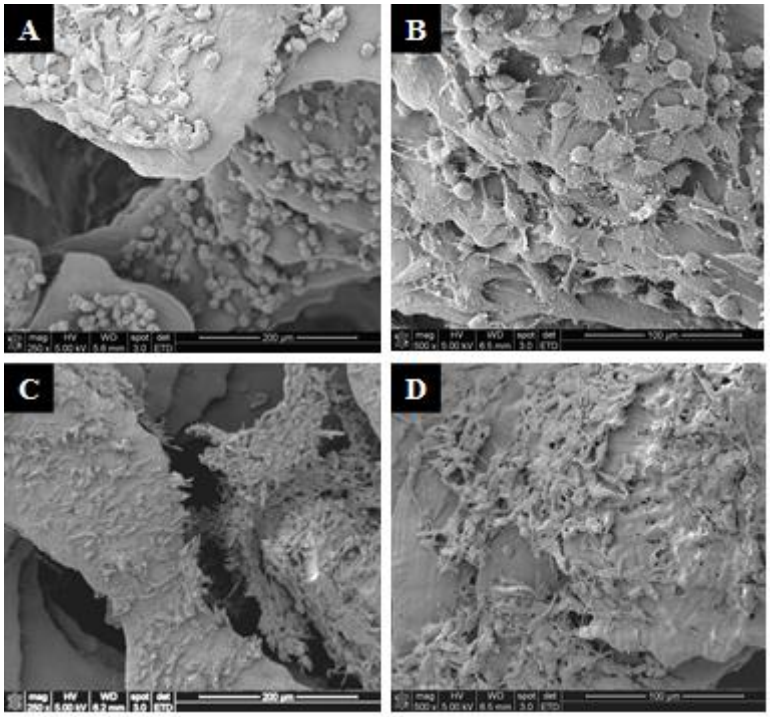

Figure 9. Validation of 3D printed PPF scaffold seeding, spreading and coating via BM-hMSC cells. At day 0 time point, cells mostly show rounded morphology with uniform distribution at lower magnification (A), while, some cells did show initiation of spreading upon observation at higher magnification (B). On the other hand, at day 7 time point, all the cells show uniform spreading and coating at lower (C) and higher (D) magnifications. Magnification for images A and C = 250X, and, images B and D = 500X.